

# The ABC-6 Family



1. The Periodic Building Unit (PerBU) - 2. Type of Faulting - 3. The Layer Symmetry
4. Connectivity Pattern - 5. Ordered End-Members - 6. Disordered Materials synthesized to date
7. Supplementary Information - 8. References

1. The periodic building unit (PerBU) equals the layer shown in Figure 1:

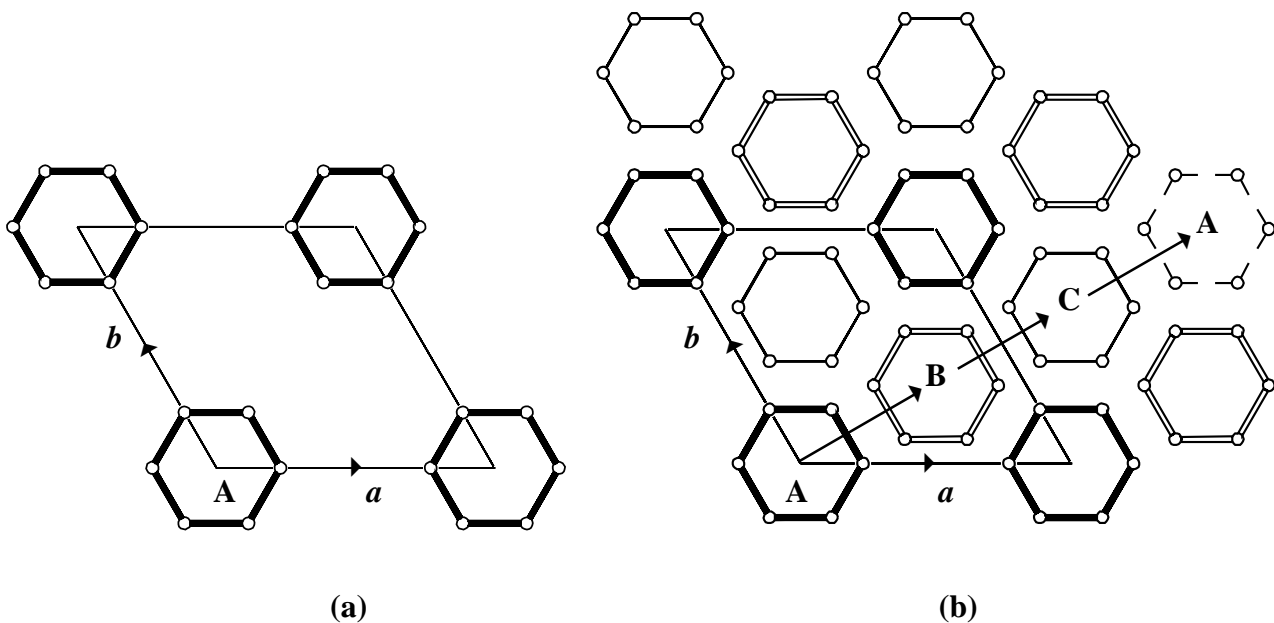


Figure 1: The PerBU is an arrangement of single T6-rings in the  $ab$ -plane of a hexagonal unit cell. In (a) a single layer, and in (b) a projection of a 3-layer stacking sequence ABC is shown

The PerBU in the ABC-6 family of framework types consists of a hexagonal array of non-connected planar T6-rings (depicted in Fig.1a in bold), which are related by pure translations along  $a$  and  $b$ . The T6-rings are centered at (0,0) in the  $ab$  layer. This position is usually called the A position (Fig.1b).



2. **Type of faulting:** 1-dimensional stacking disorder of the PerBU's along [001].



3. **The plane space group** of the PerBU is  $P(6)mm$ .



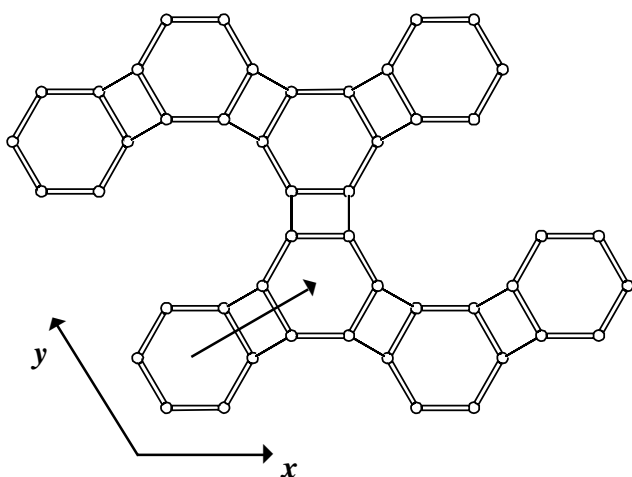
#### 4. Connectivity pattern of the PerBU:

Neighbouring PerBU's can be connected through tilted 4-rings along  $+[001]$  in three different ways:

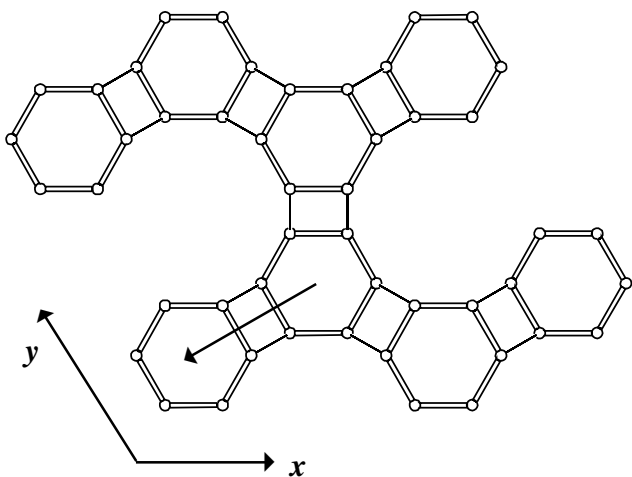
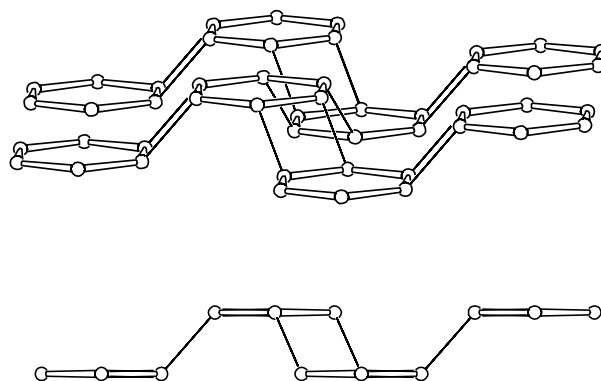
**(a):** the second layer is shifted by  $+(2/3\mathbf{a} + 1/3\mathbf{b})$  before connecting it to the first layer; so the T6-rings in the second layer are centered at  $(2/3, 1/3)$ . This position is usually denoted as the B position (Fig. 1b). The same connection mode can be repeated to generate a third PerBU shifted with respect to the second layer by (again)  $+(2/3\mathbf{a} + 1/3\mathbf{b})$ . The T6-rings are now centered at  $(4/3, 2/3)$  [or, equivalently, at  $(1/3, 2/3)$ ]. This position is called the C position (See Fig. 1b). Adding a fourth layer with the same connection mode gives a shift with respect to the first layer of  $(2\mathbf{a} + \mathbf{b})$  [or zero, i.e. the A position again]. The resulting stacking sequences, exhibiting the same connection mode, are denoted as AB, BC and CA, respectively. The connection mode is illustrated in Fig. 2a viewed down  $[001]$  (left), nearly along  $[010]$  (top right), and along  $[010]$  (bottom right).

**(b):** the second and third layers are shifted by  $-(2/3\mathbf{a} + 1/3\mathbf{b})$  before connecting them along  $+[001]$  to the previous layer to give stacking sequences AC, CB and BA. The connection modes are the same and illustrated in Fig. 2b.

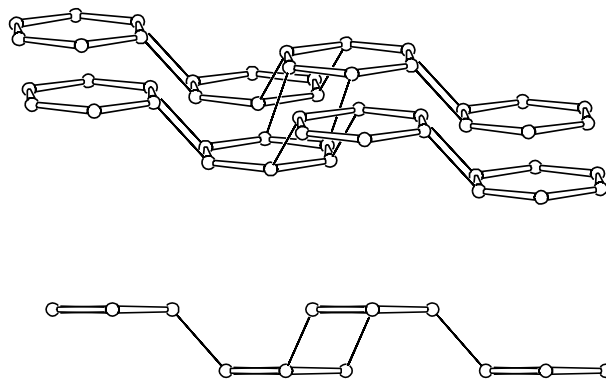
**(c):** the second layer has a zero lateral shift along  $\mathbf{a}$  and  $\mathbf{b}$ . This connection mode leads to an AA, BB or CC stacking sequence depending on whether the added layer is connected to a layer with T6-rings in the A, B or C position, respectively. The connection mode is shown in Fig. 2c.



(a)



(b)



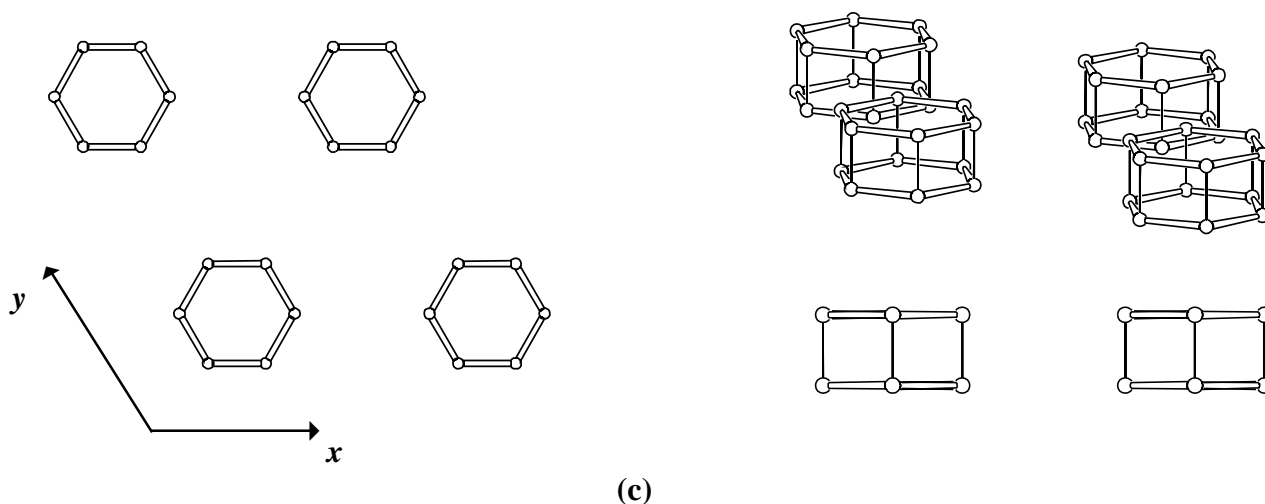


Figure 2: Connectivity modes in the ABC-6 family of zeolites

Once the stacking sequence along [001] is known, the 3-dimensional framework is defined.

Examples of faulted frameworks in the ABC-6 family of zeolites:

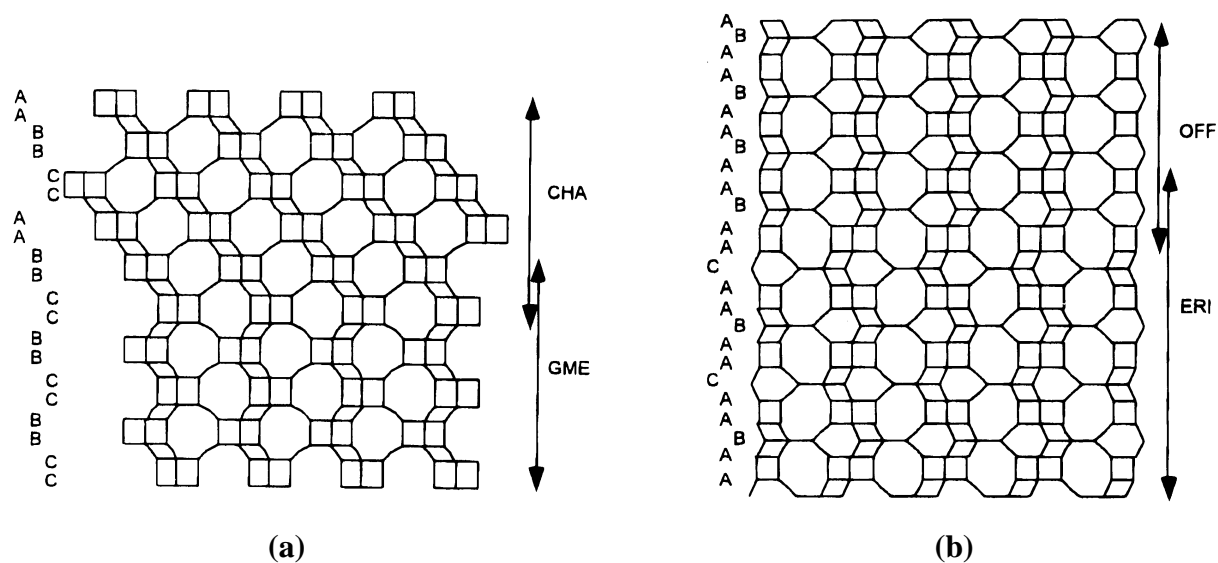


Figure 3: Examples of stacking disorder with **CHA/GME** (a) and **OFF/ERI** (b) sequences

### 5. The simplest ordered end-members in the ABC-6 family:

<i>Name</i>	<i>Code</i>	<i>#Repeat layers</i>	<i>Stacking sequence</i>
Cancrinite (1)	CAN	2	AB(A).....
Sodalite (2)	SOD	3	ABC(A).....
Losod (3)	LOS	4	ABAC(A)...

cont'd on next page

<i>Name</i>	<i>Code</i>	<i>#Repeat layers</i>	<i>Stacking sequence</i>
Liottite (4)	LIO	6	ABACAC(A).....
Afganite (5)	AFG	8	ABABACAC(A).....
Franzinite (6)	FRA	11	ABCABACABC(A).....
Offretite (7)	OFF	3	AAB(A).....
Erionite (8)	ERI	6	AABAAC(A).....
TMA-E(AB)(9)	EAB	6	AABCCB(A).....
Levyne (10)	LEV	9	AABCCABBC(A).....
STA-2 (11)	SAT	12	AABABBCBCCAC(A).....
Gmelinite (12)	GME	4	AABB(A).....
Chabazite (13)	CHA	6	AABBCC(A).....
SAPO-56 (14)	AFX	8	AABBCCBB(A).....
AIPO-52 (15)	AFT	12	AABBCCBBAACC(A).....

Examples of ordered end-members in the ABC-6 family are presented in Figure 4 in the same sequence as in the Table above.

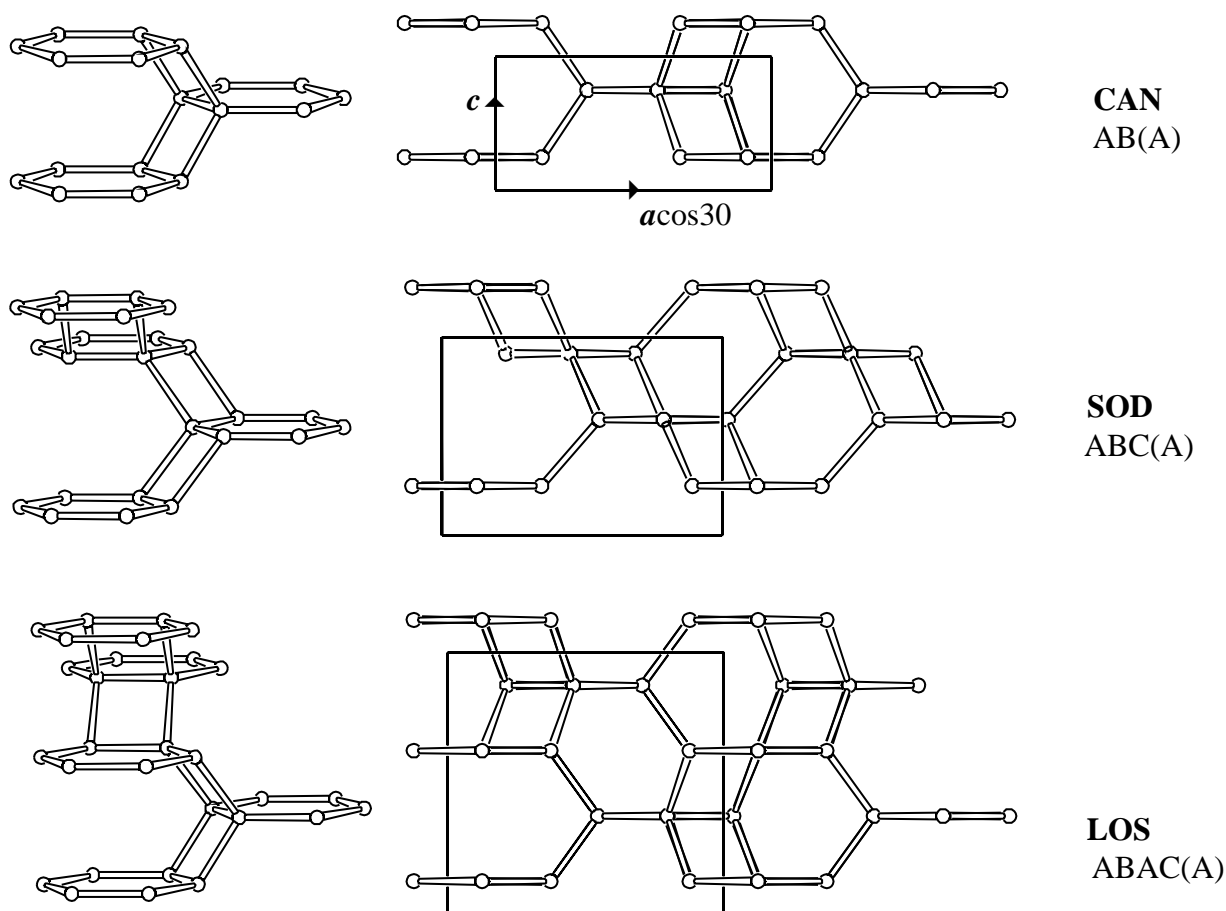
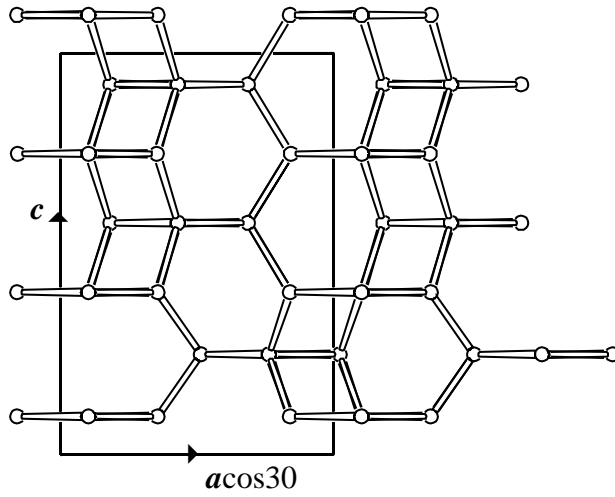
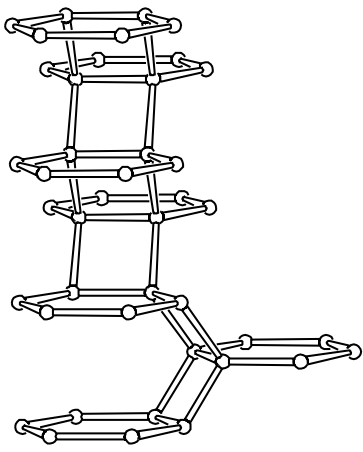
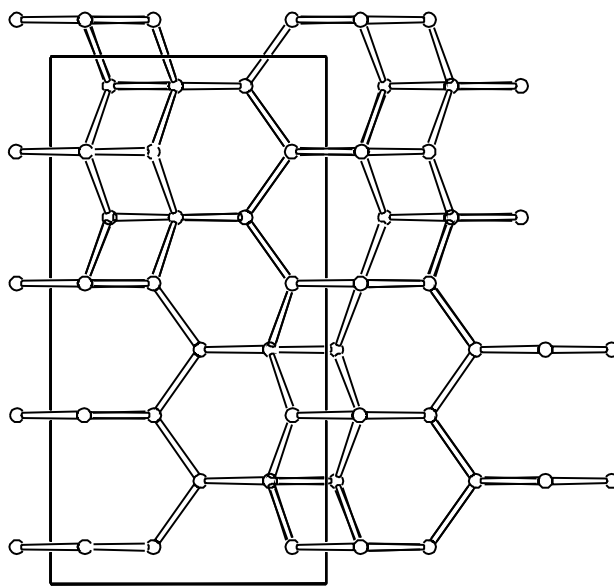
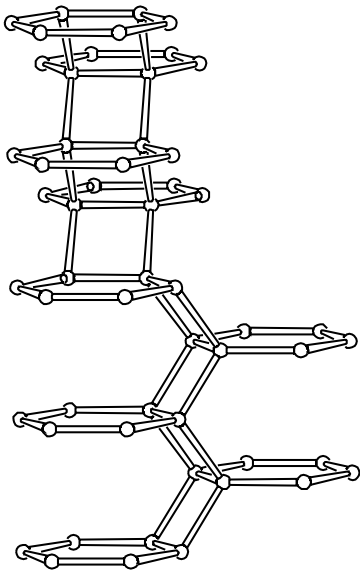


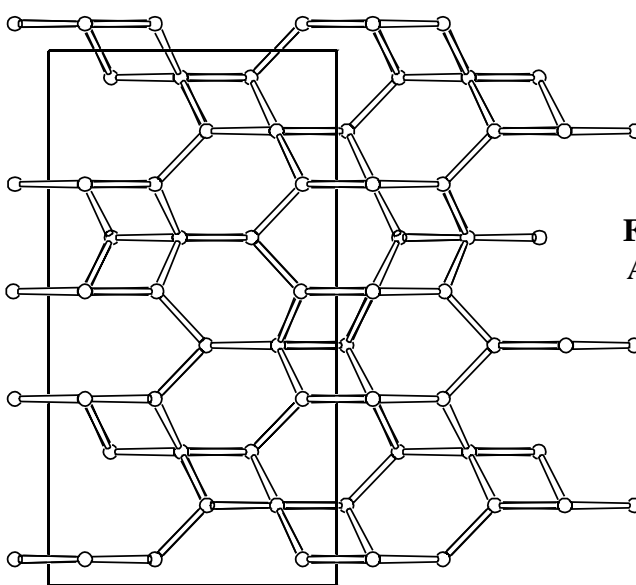
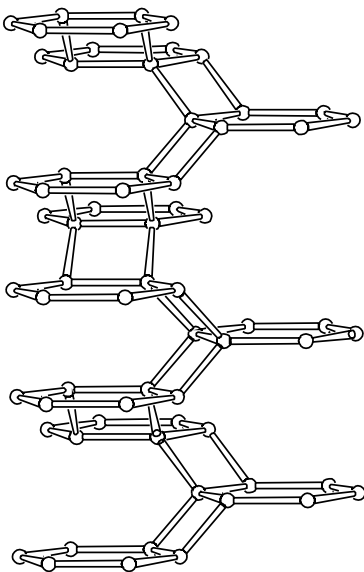
Figure 4: Perspective drawing (left) and parallel projection along [010] of the unit cell content (right) of periodic end-members in the ABC-6 family. The hexagonal  $c$  axis points towards the top of the page and the horizontal axis is equal to  $a\cos 30$  as indicated for CAN. (Fig.4 is cont'd on next page)



**LIO**  
ABACAC(A)



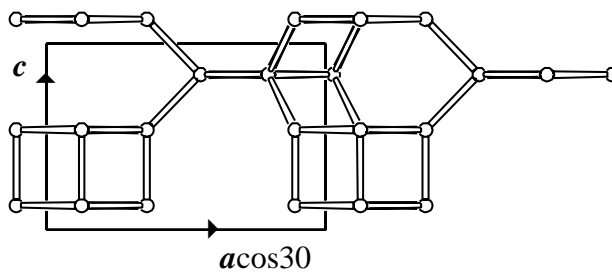
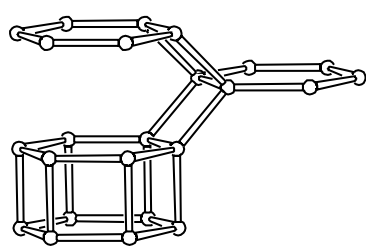
**AFG**  
ABABACAC(A)



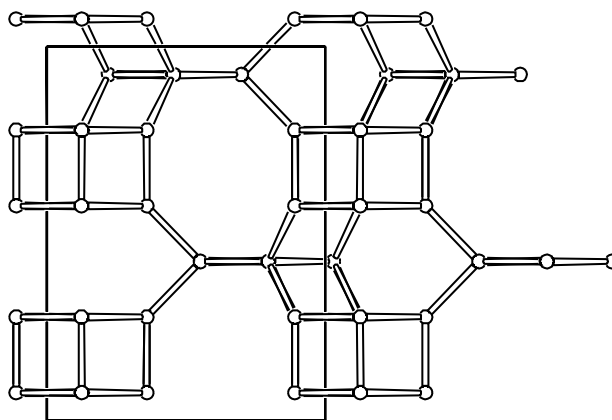
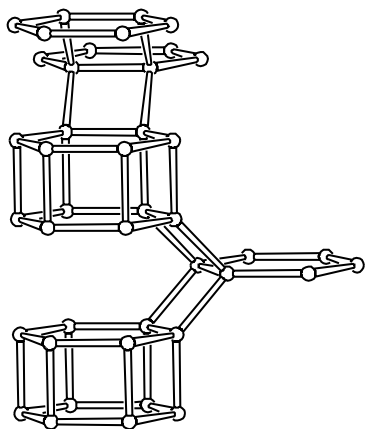
**FRA**  
ABCABACABC(A)

Figure 4 (Continued): For legend: See previous page. (Fig.4 is continued on next page)

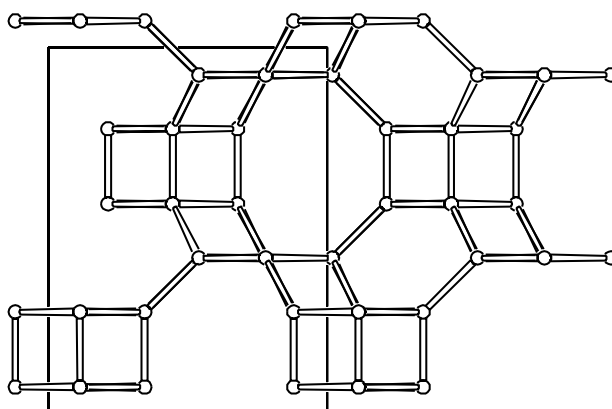
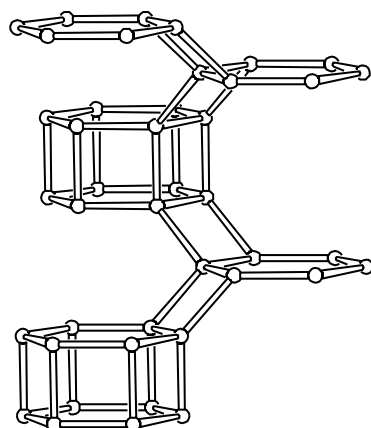




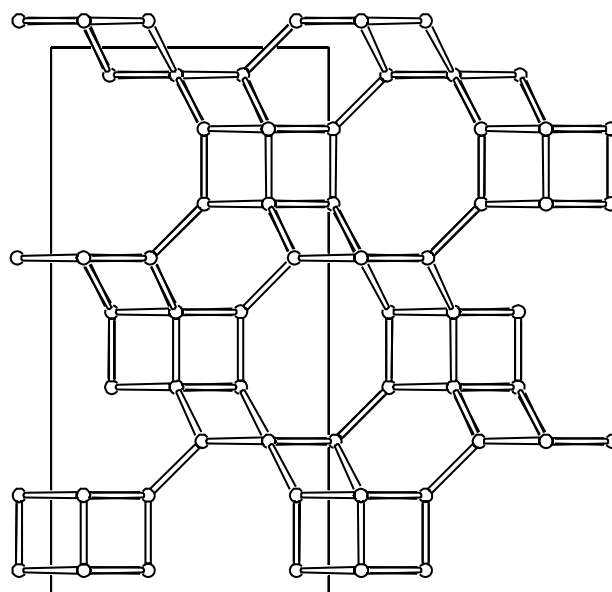
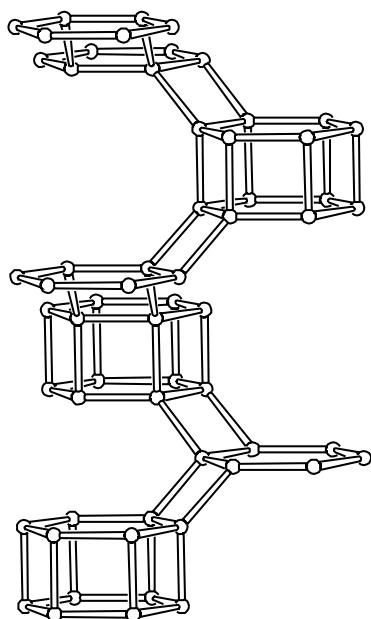
**OFF**  
AAB(A)



**ERI**  
AABAAC(A)



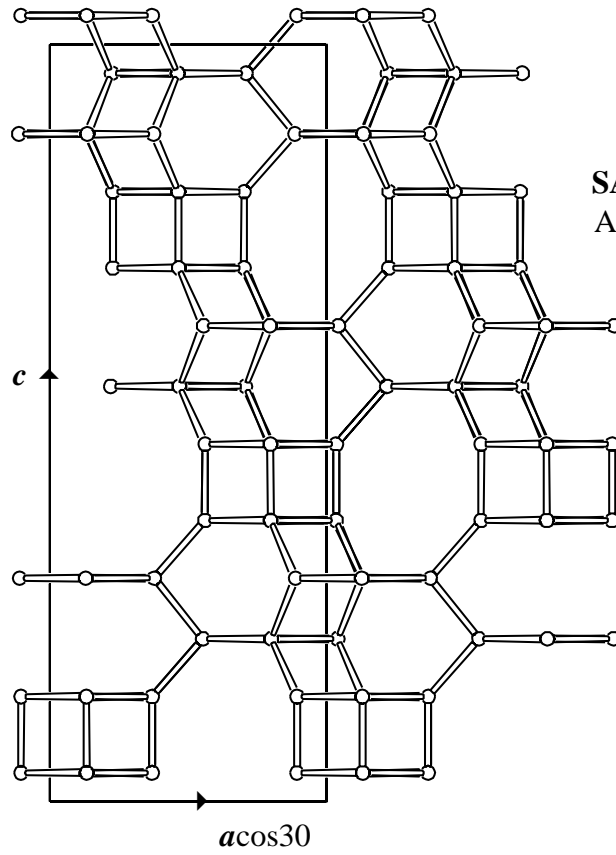
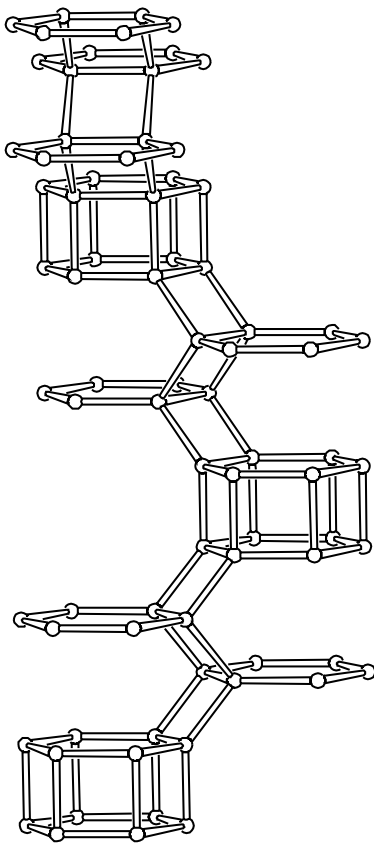
**EAB**  
AABCCB(A)



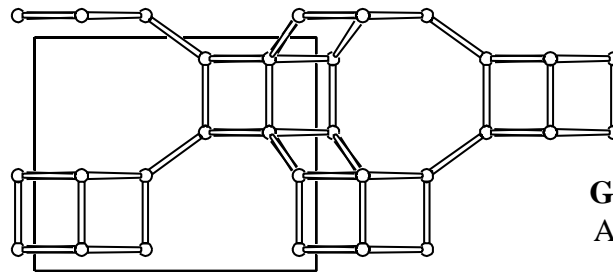
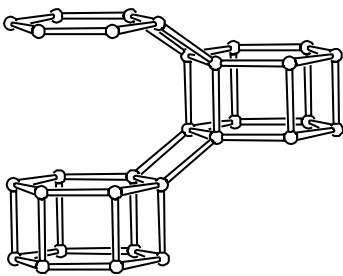
**LEV**  
AABCCABBC(A)

Figure 4 (Continued): For legend: See next page. (Fig.4 is continued on next page)

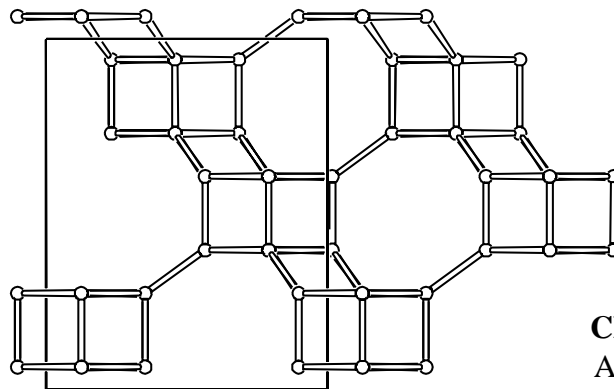
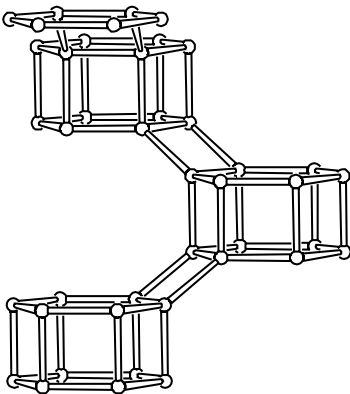




**SAT**  
AABABBCBCCAC(A)



**GME**  
AABB(A)



**CHA**  
AABBCC(A)

Figure 4 (Continued): Perspective drawing (left) and parallel projection along [010] of the unit cell content (right) of periodic end-members in the ABC-6 family. The hexagonal  $c$  axis points towards the top of the page; the horizontal axis is equal to  $a\cos 30$ . (Fig.4 is continued on next page)



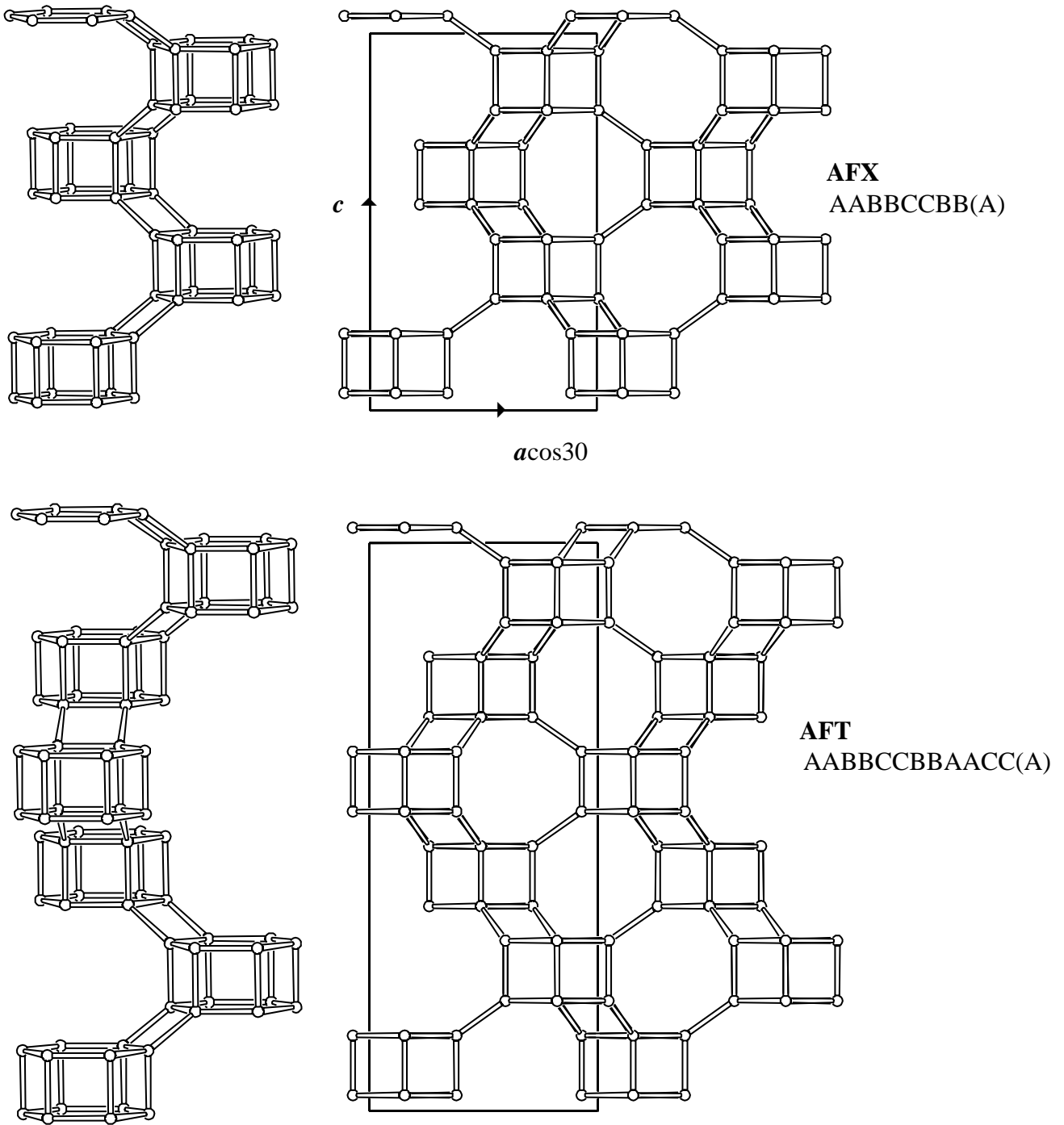


Figure 4 (Continued): Perspective drawing (left) and parallel projection along [010] of the unit cell content (right) of periodic end-members in the ABC-6 family. The hexagonal  $c$  axis points towards the top of the page; the horizontal axis is equal to  $a\cos 30$ . (Final page of Figure 4)



## 6. Disordered materials synthesized and characterized to date:

Linde T (ERI/OFF) (16); Babelite (random stacking) (17); Linde D (disordered CHA) (18); Phi (disordered CHA) (19); ZK-14 (disordered CHA) (20); LZ-276 (disordered CHA) (21); LZ-277 (disordered CHA) (21).



## 7. Supplementary material

Since the ABC-6 family contains 15 ordered end-members simulations of powder patterns for stacking disorder of only the most common framework types are given.

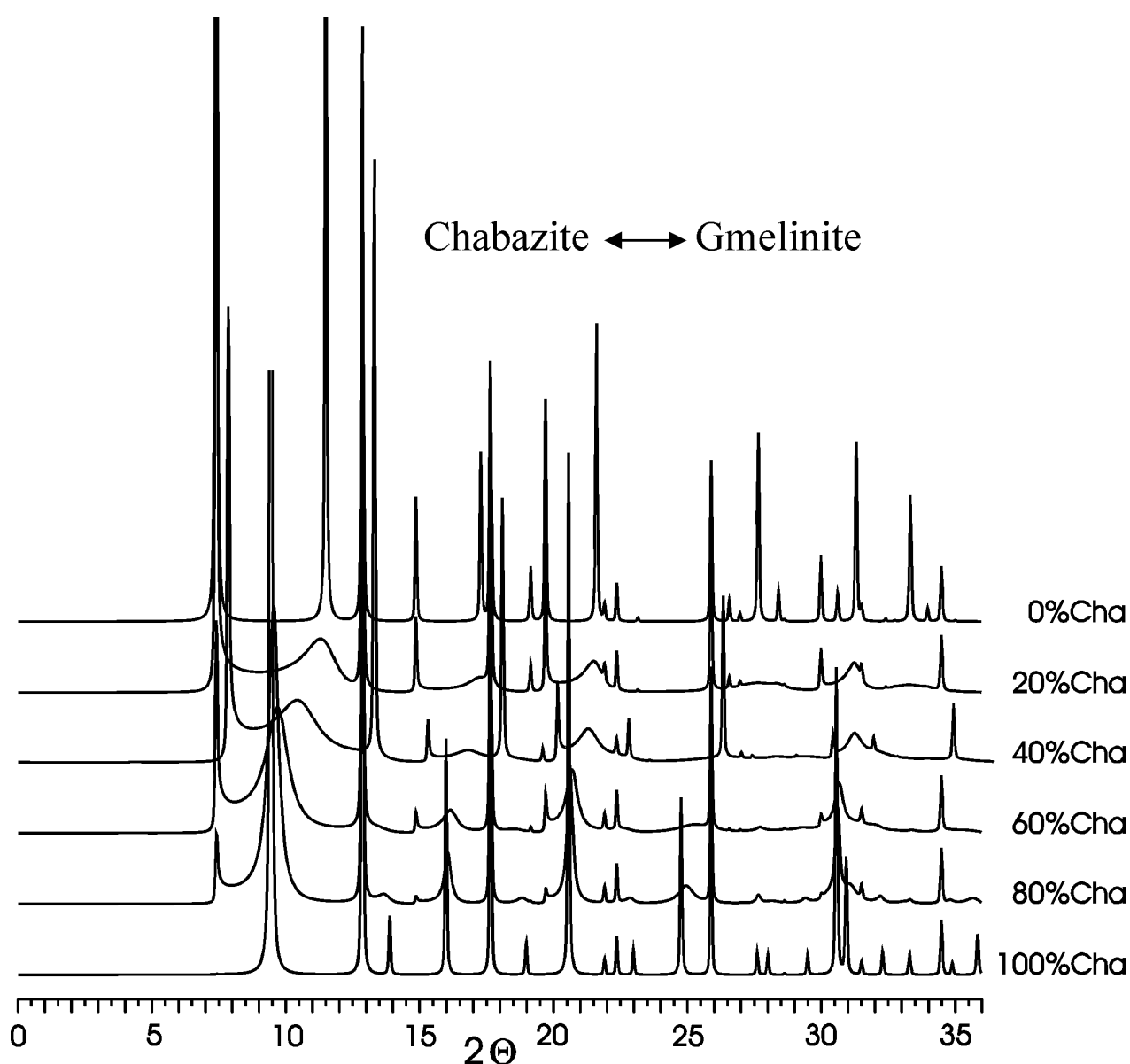


Figure 5: Simulated powder pattern of the Gmelinite/Chabazite series. In this example, the stacking of the PerBU's in AAB- and AABCC-sequences is disordered



### Simulation of the stacking disorder in the ABC-6 family: ERI-OFF

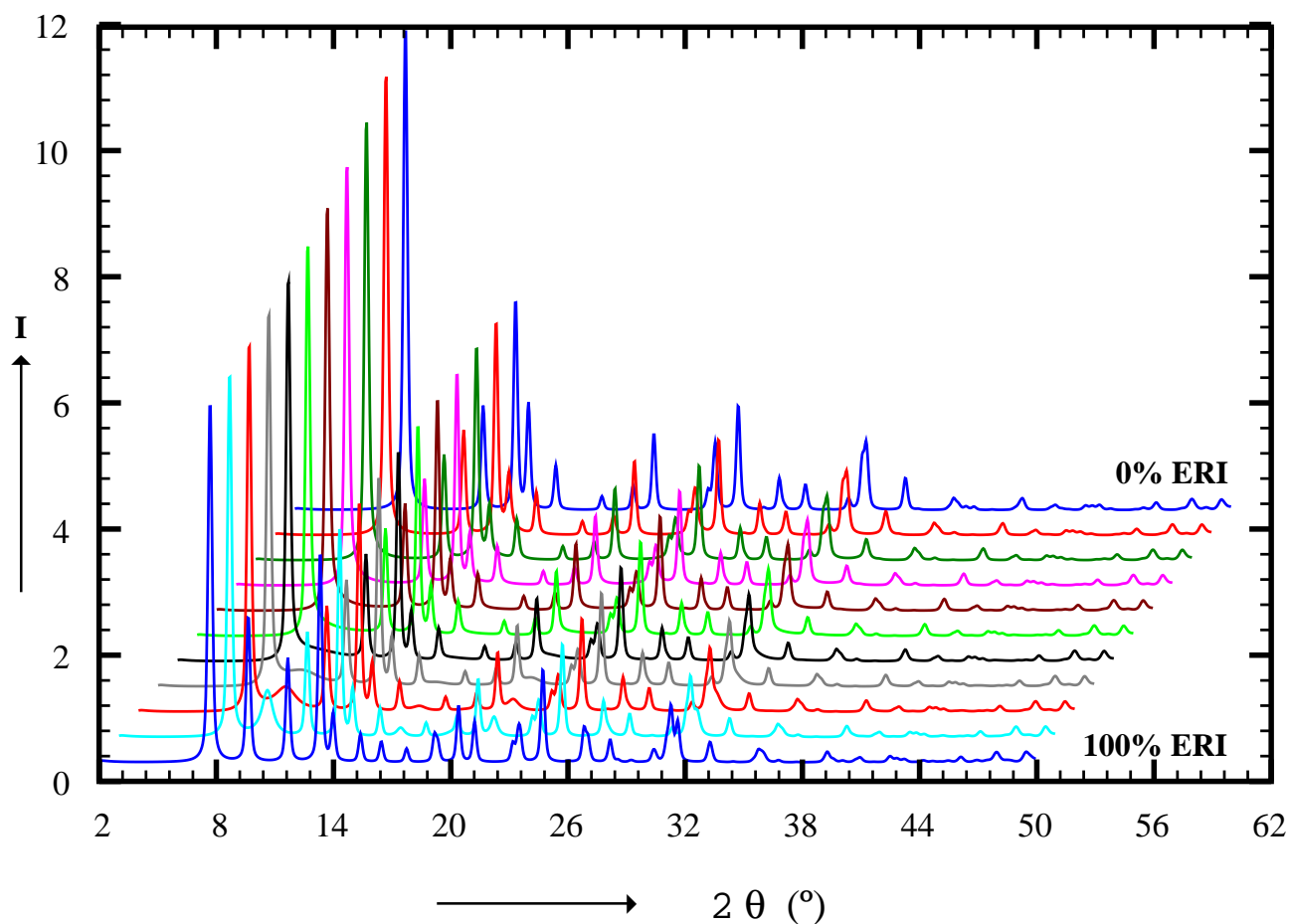


Figure 6: Intensity (I, a.u.) of simulated powder patterns versus diffraction angle ( $2\theta$ ) of the ERI-OFF series in steps of 10% intergrowth. The stacking sequences of ERI and OFF are disordered. The 0% ERI pattern corresponds to the 100% OFF pattern



## 8. References

- (1) a) L. Pauling, Proc. Natl. Acad. Sci. **16**, 453 (1930).  
b) O. Jarchow, Z. Kristallogr. **122**, 407 (1965).
- (2) a) L. Pauling, Z. Kristallogr. **74**, 213 (1930).  
b) J. Loens and H. Schulz, Acta Cryst. **23**, 434 (1967).
- (3) W. Sieber and W.M. Meier, Helv. Chim. Acta **57**, 1533 (1974).
- (4) S. Merlino and P. Orlandi, Am. Mineral. **62**, 321 (1977).
- (5) P. Bariand, F. Cesbron and R. Giraud, Bull. Soc. Fr. Mineral. Cristallogr. **91**, 34 (1968).
- (6) P. Ballirano, E. Bonaccorsi, A. Maras and S. Merlino, Can. Mineral. **38**, 657 (2000).
- (7) J.M. Bennett and J.A. Gard, Nature **214**, 1005 (1967).
- (8) L.W. Staples and J.A. Gard, Mineral. Mag. **32**, 261 (1959).
- (9) R. Aiello and R.M. Barrer, J. Chem. Soc. A **1970**, 1470 (1970).
- (10) R.M. Barrer and I.S. Kerr, Trans. Farad. Soc. **55**, 1915 (1959).
- (11) G.W. Noble, P.A. Wright and Å. Kvik, J. Chem. Soc. Dalton Trans. **23**, 4485 (1997).
- (12) K. Fischer, N. Jb. Miner. Mh. **1966**, 1 (1966).
- (13) a) L.S. Dent and J.V. Smith, Nature **181**, 1794 (1958).  
b) J.V. Smith, R. Rinaldi and L.S. Dent, Acta Cryst. **16**, 45 (1963).
- (14) a) S.T. Wilson, N.K. McGuire, C.S. Blackwell, C.A. Bateman, and R.M. Kirchner. In: *Zeolite Science 1994: Recent Progress and Discussions*. Studies in Surface Science and Catalysis, Vol. 98. Elsevier Science B.V., 1995, p 9.  
b) R.F. Lobo, S.I. Zones and R.C. Medrud, Chem. Mater. **8**, 2409 (1996).
- (15) a) J.M. Bennett, R.M. Kirchner and S.T. Wilson. In: Proc. 8th IZC, *Zeolites: Facts, Figures, Future*. P.A. Jacobs and R.A. van Santen (eds.). Elsevier Science Publishers B.V., Amsterdam, 1989, p 731.  
b) N.K. McGuire, C.A. Bateman, C.S. Blackwell, S.T. Wilson and R.M. Kirchner, *Zeolites* **15**, 460 (1995).
- (16) D.W. Breck, *Zeolite Molecular Sieves*. Wiley, 1974, p 173.
- (17) R. Szostak and K.P. Lillerrud, J. Chem. Soc. Chem. Commun. **1994**(20), 2357 (1994).
- (18) K.P. Lillerud, R. Szostak and A. Long, J. Chem. Soc. Faraday Trans. **90**, 1547 (1994).
- (19) K.P. Lillerud, R. Szostak and A. Long, J. Chem. Soc. Faraday Trans. **90**, 1547 (1994).
- (20) G.H. Kuehl. In: *Molecular Sieves*. S.C.I., London, 1967, p 85.

- (21) G.W. Skeels, M. Sears, C.A. Bateman, N.K. McGuire, E.M. Flanigen, M. Kumar and R.M. Kirchner, *Micropor. Mesopor. Mater.* **30**, 335 (1999).

